Chang Yi Wang[1, 2]
Chien C. Chang[1, 3]

[1]Division of Mechanics, Research Center for Applied Sciences, Academia Sinica, Taipei, Taiwan
[2]Departments of Mathematics and Mechanical Engineering, Michigan State University, East Lansing, MI, USA
[3]Institute of Applied Mechanics, National Taiwan University, Taipei, Taiwan

Received January 2, 2007
Revised March 12, 2007
Accepted March 13, 2007

Research Article

EOF using the Ritz method: Application to superelliptic microchannels

An efficient Ritz method is developed from the variational principle to solve the Poisson–Boltzmann equation under the Debye–Hückel approximation for studying the EOF in microchannels. The method is applied to the family of superelliptic cross sections which includes the elliptic channel and the rectangular channel as limiting cases. Several accurate tables presented are useful for design of electroosmotic channels, especially rectangular channels with rounded corners. It is shown how the flow rate Q is a sophisticated consequence of the nondimensional electrokinetic width K, the aspect ratio b as well as the superelliptic exponent n.

Keywords:
Debye–Hückel approximation / EOF / Ritz method / Superelliptic
DOI 10.1002/elps.200700001

1 Introduction

Microfluidics has become extremely important in biotechnology [1]. One method to generate flow in minute conduits is through electroosmosis, where a fluid adjacent to electrostatically charged surfaces moves under an applied electric field [2, 3]. For parallel steady flow caused solely by electroosmosis in a tube, the fluid velocity is governed by the reduced Navier–Stokes equation

$$\nabla^2 w = -\frac{\rho_\varepsilon E}{\mu} \tag{1}$$

where w is the longitudinal fluid velocity, μ the fluid viscosity, E the longitudinal applied electric field, and ρ_e is the charge density which can be expressed by a potential distribution ψ

$$\rho_e = -\varepsilon \nabla^2 \psi = -2zen_0 \sinh\left(\frac{ze\psi}{k_b T}\right) \tag{2}$$

where ε is the dielectric constant of the medium, z the valence, e the electron charge, n_0 the bulk electrolyte concentration, k_b the Boltzmann constant, and T is the temperature. Equation (2) is the nonlinear Poisson–Boltzmann equation. The boundary conditions are that the velocity is 0 and a constant potential ψ_0 is given on the wall of the channel.

If the electrical potential is small compared to the thermal energy of ions, the ratio $(ze\psi_0/k_bT)$ is much less than 1. Let $\phi = \psi/\psi_0$ and normalize all the lengths by the half width of the channel L. Equation (2), under the Debye–Hückel approximation, is linearized to

$$\nabla_0^2 \phi = K^2 \phi \tag{3}$$

where we have the normalized Laplace operator $L^2\nabla^2 = \nabla_0^2 = \partial^2/\partial x^2 + \partial^2/\partial y^2$ with x and y the normalized Cartesian coordinates, and have defined $K^2 = (\kappa L)^2 = 2z^2e^2n_0L^2/(\varepsilon k_bT)$. K is called the nondimensional electrokinetic width and κ the Debye–Hückel parameter. Now $\phi = 1$ on the boundary, and then from Eqs. (1) and (3), we have the induced velocity

$$w = -\frac{\varepsilon\psi_0 E}{\mu}(1 - \phi) \tag{4}$$

Analytical solution for the Poisson–Boltzmann equation only exists for the parallel plate channel (see, *e.g.*, [4]). Analytical solutions for the simpler Eq. (3) under Debye–Hückel approximation include circular cross section [5], and the rectangular cross section (in infinite series; [6–8]). Simply derived analytical solutions are given in the Appendix. For all other cross sections, numerical methods such as finite elements [9] or boundary collocation [10] must be used.

The purpose of this paper was to study the EOF in superelliptic channels. For this, we shall develop a powerful Ritz method for EOFs. These cross-sectional shapes represents rectangular channels with rounded corners, and include the rectangular channel and the elliptic channel as limiting cases. In practice, an etched rectangular channel seldom has sharp corners and thus the cross-sectional shape may be well represented by a superellipse studied in this paper.

Correspondence: Professor Chien C. Chang, Institute of Applied Mechanics, National Taiwan University, Taipei 106, Taiwan
E-mail: mechang@gate.sinica.edu.tw
Fax: +886-2-23625238

2 The Ritz method

The Ritz method is best known for solving eigenvalue problems, but it can be applied to boundary value problems as well [11]. The variational principle shows that Eq. (3) is equivalent to the minimization of the integral

$$J = \iint (\phi_x^2 + \phi_y^2 + K^2\phi^2)\, dxdy \tag{5}$$

where the integration is over the cross-sectional area. Let ϕ be approximated by

$$\phi = 1 - \sum c_i f_i(x, y) \tag{6}$$

where c_i are coefficients to be determined, and f_i is a complete sequence of base functions (actually polynomials) each being 0 on the boundary. Substituting Eq. (6) into Eq. (5) and using the necessary condition for extremum

$$\frac{\partial J}{\partial c_i} = 0 \tag{7}$$

yields

$$\sum_{j=1}^{N} A_{ij} c_j = K^2 B_i, \quad I = 1 \text{ to } N \tag{8}$$

Here we have truncated the series to N terms, and

$$A_{ij} = \iint (f_{ix} f_{jx} + f_{iy} f_{jy} + K^2 f_i f_j)\, dxdy,$$
$$B_i = \iint f_i\, dxdy \tag{9}$$

Since the base functions f_i are prescribed, A_{ij} and B_i can be readily computed. Hence, Eqs. (8) and (9) constitute a system of algebraic equations for c_j, which can be solved by any standard solver for linear systems. The flow velocity is obtained as

$$w = -\frac{\varepsilon\psi_0 E}{\mu} \sum_{1}^{N} c_i f_i \tag{10}$$

Later, we will use $\bar{w}$ to denote the flow velocity normalized by $-\varepsilon\psi_0 E/\mu$. Integrating w over the cross section gives the flow rate

$$Q = -\frac{\varepsilon\psi_0 E L^2}{\mu} \sum_{1}^{N} c_i B_i \tag{11}$$

In the following discussion, we often use $\bar{Q}$, the flow rate normalized by $-\varepsilon\psi_0 E L^2/\mu$.

3 Results for superelliptic channel

A superelliptic shape of normalized width 2 and height 2b (b is the aspect ratio < 1) is given by

$$1 - x^{2n} - (y/b)^{2n} = 0 \tag{12}$$

It is an ellipse when $n = 1$ and approaches a rectangle when $n \to \infty$. Figure 1 shows some of the shapes. The Ritz method has been applied to the vibration and buckling of a superelliptic plates [12] but has not previously been applied to flow problems.

Since the problem is symmetrical, we choose the sequence

$$\{f_i\} = \left[1 - x^{2n} - \left(\frac{y}{b}\right)^{2n}\right] \times$$
$$\times \{1, x^2, y^2, x^4, x^2y^2, y^4, x^6, x^4y^2, x^2y^4, y^6, \cdots\} \tag{13}$$

The number of terms taken may be $N = 1, 3, 6, 10, 15, 21,$ *etc.,* to include the highest homogeneous powers. The series is absolutely convergent within a square $|x, y| \leq 1$. Let us compare the exact solution for a circular channel (Eq. A3) to our Ritz solution ($b = 1$). Table 1 shows the results.

We see that the convergence is fairly fast. In general, $N = 15$ is adequate for a four-digit accuracy. The elliptic channel is described by $n = 1$. Table 2 shows our results.

The elliptic cross section was also studied by Hsu *et al.* [13], but no numerical values are presented, and thus cannot be compared with our results. The results for superelliptic channels are given in Tables 3–5.

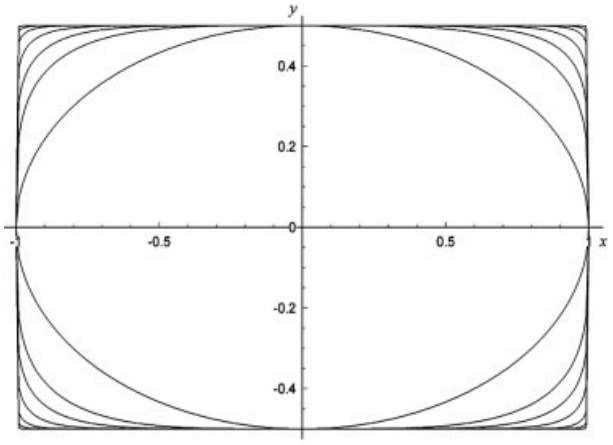

Figure 1. Superelliptic shapes ($b = 0.5$) with $n = 1, 2, 3, 5, 10, 20, 50$ from inside.

Table 1. Accuracy of the normalized flow rate $\overline{Q}$ for the circular cross section

N/*K*	0.1	1	10
3	0.003920	0.33684	2.5071
6	0.003920	0.33684	2.5428
10	0.003920	0.33684	2.5455
15	0.003920	0.33684	2.5456
Exact	0.003920	0.33684	2.5456

Table 2. The normalized flow rate $\overline{Q}$ for the elliptic cross section ($n = 1$), where the solutions in the last column are obtained from Eq. (A3)

K/b	0.25	0.5	0.75	1
0.1	0.000116	0.000785	0.00212	0.00392
0.2	0.000462	0.00313	0.00844	0.0156
0.5	0.00287	0.0193	0.0515	0.0943
1	0.0133	0.0736	0.189	0.337
2	0.0429	0.249	0.576	0.950
5	0.195	0.757	1.39	2.02
10	0.405	1.12	1.84	2.55
20	0.580	1.34	2.09	2.84
50	0.701	1.47	2.25	3.01
∞	0.7854	1.571	2.356	3.142

Table 3. Effects of n and b on the normalized flow rate $\overline{Q}$ for $K = 0.1$, where we used Eq. (A8) for the rectangular channel ($n = \infty$)

n/b	0.25	0.5	0.75	1
1	0.000116	0.000785	0.00212	0.00392
2	0.000159	0.00106	0.00283	0.00523
5	0.000174	0.00113	0.00302	0.00558
10	0.000175	0.00114	0.00304	0.00561
∞	0.000176	0.00114	0.00304	0.00561

Table 4. Effects of n and b on the normalized flow rate $\overline{Q}$ for $K = 1$, where we used Eq. (A8) for the rectangular channel ($n = \infty$)

n/b	0.25	0.5	0.75	1
1	0.0133	0.0736	0.189	0.337
2	0.0155	0.0983	0.249	0.441
5	0.0170	0.1055	0.266	0.469
10	0.0171	0.1061	0.267	0.471
∞	0.0172	0.1062	0.267	0.472

Table 5. Effects of n and b on the normalized flow rate $\overline{Q}$ for $K = 10$, where we used Eq. (A8) for the rectangular channel ($n = \infty$)

n/b	0.25	0.5	0.75	1
1	0.405	1.120	1.836	2.546
2	0.512	1.355	2.199	3.039
5	0.550	1.438	2.330	3.221
10	0.554	1.449	2.347	3.245
∞	0.555	1.451	2.351	3.251

We see that the flow rate is bounded between the ellipse ($n = 1$, Table 2) and the rectangle ($n = \infty$, Table A1). Typical distributions of the normalized velocity $\bar{w}$ are shown in Fig. 2. The boundary layer nature of high K is evident.

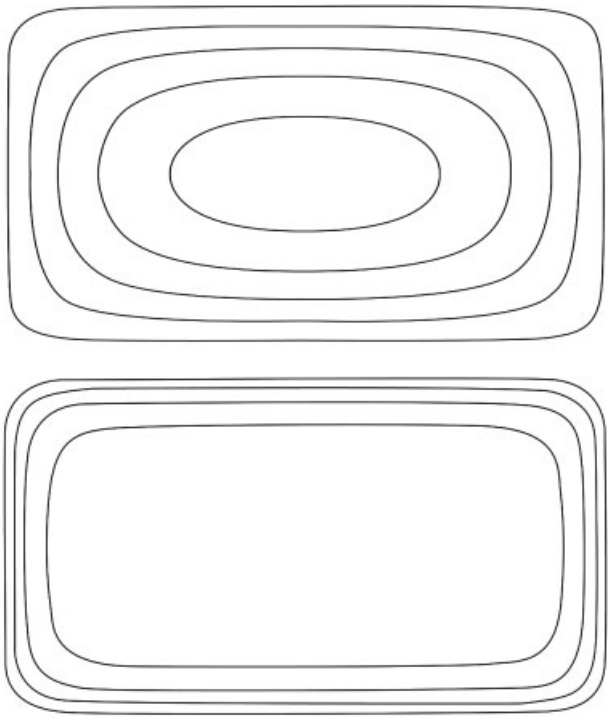

Figure 2. Velocity distributions for $b = 0.5$, $n = 5$. Top: $K = 0.1$, value between curves $\Delta\bar{w} = 0.00025$. Bottom: $K = 10$, $\Delta\bar{w} = 0.25$.

Some channels are in the shape of a semisuperellipse, *i.e.*, half of the shape in Fig. 1. Instead of extensive tables, we shall briefly describe how the Ritz method can be applied. Let the midline $y = 0$ be a boundary and consider only the upper half. Since there is no symmetry in the y direction, Eq. (13) is supplanted by

$$\{f_i\} = y\left[1 - x^{2n} - \left(\frac{y}{b}\right)^{2n}\right]\times \times\left\{1, y, x^2, y^2, y^3, x^4, x^2y^2, y^4, y^5, x^6, x^4y^2, x^2y^4, y^6, \cdots\right\} \quad (14)$$

Note that $f_i = 0$ on the boundary. Take first N of these elements, where N may be 4, 5, 8, 9, 13, 14, *etc.* As in Table 1, N is determined by the acceptable accuracy. Then the area integrals of Eq. (9) are computed. For example

$$A_{11} = 2\int_0^1\int_0^{y_1}\left[\left(\frac{\partial f_1}{\partial x}\right)^2 + \left(\frac{\partial f_1}{\partial y}\right)^2 + K^2 f_1^2\right] dy dx \quad (15)$$

where from Eq. (12)

$$y_1 = b(1 - x^{2n})^{1/2n} \quad (16)$$

Due to the fact that f_i are polynomials, the inner integral can be integrated exactly and the outer integral can be evaluated numerically by quadratures. Then Eq. (8) is solved for c_i by a

simple inversion program. The velocity and flow rate are given by Eqs. (10) and (11).

4 Discussion

If there were an additional pressure gradient, Eq. (1) would have a nonhomogeneous pressure term on the right-hand side. However, Eq. (1) is linear, and the flow due to pressure (which is not considered in this paper) can be superposed. Note that the direction of EOF can be reversed, by reversing either the surface charge ψ_0 or the applied electric field E.

Our Ritz method is simple and efficient. Its derivation presented here is facilitated by a similar Ritz method applied on the better known Helmholtz equation, which differs by a sign from Eq. (3) (Debye–Hückel approximation). The present problem can also be solved by other methods of numerical integration such as finite-difference and finite-element methods. However, the small radii of the corners would present severe challenges for these methods. Since the Ritz method is boundary fitted, there are no difficulties in the corner regions.

In general, the normalized flow rate $\bar{Q}$ increases with increase in K, but the increase is slow for very small or very large values of K. With other factors being fixed, K is proportional to the half channel width L, while the dimensional flow rate Q is proportional to $\bar{Q}L^2$. For example, consider the circular channel. Figure A1 shows the normalized flow rate $\bar{Q}$ as the function of K. If K is small, the dimensional flow rate Q has a fourth-power dependence upon L as $\bar{Q} \sim K^2$ (*cf.* Eq. A4). If K is large, Q will have a second-power dependence upon L since $\bar{Q}$ approaches π for large K (*cf.* Eq. A5). The similar behaviors hold for other geometries. For example, consider the elliptic channel ($n = 1$). Looking into $\bar{Q}$ of the first two rows (small K) of Table 2, we see that $Q/L^4 \sim \bar{Q}/L^2 \sim \bar{Q}/K^2$ is very close to a constant for each given aspect ratio b.

Now, we examine the effects of the aspect ratio $b < 1$. Tables 2–5 and A1 show that if we increase b (with other factors being fixed), the flow rate (either dimensional or normalized) is increased. The increase is most significant for small K, but is still substantial for moderately large K. Consider again the elliptic cross section. At $K = 0.1$, the flow rate for $b = 1$ is 33.8 times that for $b = 0.25$, though the area is only increased by the factor 4. As a comparison, at $K = 1$ the increase in the flow rate is 25.3 times, while at $K = 10$, the increase is only 6.29 times.

Next, we fix the cross-sectional area with other factors being unchanged. The effect of the aspect ratio b is more complicated, since an increase in b would decrease L and K, and thus affect the flow rate. Let us consider elliptic channels for which the cross-sectional area πbL^2 is fixed. First, take $b = 0.25$ and $K = 0.2$ with $L = 20\ \mu$m. Table 2 gives $\bar{Q} = 0.000462$, and the dimensional flow rate Q is proportional to $\bar{Q}L^2 = 0.1848\ (\mu\text{m})^2$. Next, picking up $b = 1$ and $K = 0.1$ with $L = 10\ \mu$m gives the same cross-sectional area. Table 2 shows that the latter case has $\bar{Q} = 0.00392$, and Q is represented by $\bar{Q}L^2 = 0.392\ (\mu\text{m})^2$, which is 2.121 times the previous $0.1848\ (\mu\text{m})^2$! For a further illustration, consider another example between ($b = 0.25$, $K = 1$, $L = 20\ \mu$m) and ($b = 1$, $K = 0.5$, $10\ \mu$m). Table 2 gives $\bar{Q} = 0.0133$ for the former case ($b = 0.25$, $K = 1$, $L = 20\ \mu$m), and the dimensional flow rate Q is proportional to $\bar{Q}L^2 = 5.32\ (\mu\text{m})^2$. Table 2 shows that the latter case ($b = 1$, $K = 0.5$, $L = 10\ \mu$m) has $\bar{Q}L^2 = 9.43\ (\mu\text{m})^2$, which is 1.773 times $5.32\ (\mu\text{m})^2$ for the former case. Similar results hold for other shapes of channels, such as rectangular channels. It is concluded that for the same cross-sectional area, an increase in the aspect ratio b (more rounded shape) increases the dimensional flow rate $\bar{Q}$. But the actual increase in the flow rate depends on the two states (b_1, K_1) and (b_2, K_2) one likes to compare, and in general the increase in the flow rate is more significant if one of K_1 and K_2 is small.

Tables 3–5 also allow us to examine the effect of rounding the corner by the superelliptic exponent n. First, the flow rate $\bar{Q}$ increases with increase in the superelliptic exponent n; the increase is more substantial for small K. For example at $K = 0.1$, the flow rate for the rectangular channel is 1.716 times that for the elliptic channel, while the area ratio is $4/\pi = 1.273$. Next, for small and large K (say, 0.1 and 10), the ratio of the flow rate for $b = 1$ to that for $b = 0.25$ decreases monotonically as the exponent n is increased from 1 (elliptic cross section) to infinity (rectangular channels). But in an intermediate range of K (say, 1), there is an optimal round shape that gives the highest ratio (it is $n = 2$ in Table 4). Moreover, the increase in the flow rate $\bar{Q}$ by increasing b is minimal when n is larger than 10, or, the radius of curvature is smaller than 0.07.

5 Concluding remarks

Because of the existence of the Debye layer, the dimensional flow rate Q in microchannels does not increase simply in proportion to the cross-sectional area unless the number K is infinite. The efficient Ritz method was for the first time applied to solve Eq. (3) of the Debye–Hückel approximation; the accurate solutions enable us to draw conclusive remarks on the effects of the various parameters, and the main results are summarized as follows:

(i) The dimensional flow rate Q increases with increase in the superelliptic exponent n. The increase is more substantial for small K. For example at $K = 0.1$, the flow rate for the rectangular channel is 1.716 times that for the elliptic channel, compared to the ratio of their cross-sectional areas $4/\pi = 1.273$.

(ii) The dimensional flow rate Q increases with increase in the aspect ratio b. The increase is significant for small K, and is still substantial for moderately large K. Take the elliptic channel for example. At $K = 0.1$, the flow rate for $b = 1$ is about 33.8 times that for $b = 0.25$, though the area is only increased by the factor 4. The increase at $K = 10$ for the same situation is only about 6.29 times.

(iii) If we fix the cross-sectional area with other factors unchanged, the dimensional flow rate Q is increased with increase in the aspect ratio $b < 1$ (though the half channel width L is reduced accordingly). In general, this is true. But the actual increase in the flow rate depends on the two states (b_1,K_1) and (b_2,K_2) one likes to compare, and the increase is more significant if one of K_1 and K_2 is very small.

As a final remark, in the limiting cases for rectangular channels, all the computed results are consistent with the asymptotic behaviors, obtained in the Appendix, which are derived from a much simpler series solution (A8).

6 References

[1] Stone, H. A., Stroock, A. D., Ajdari, A., *Ann. Rev. Fluid Mech.* 2004, *36*, 381–411.

[2] Probstein, R. F., *Physicochemical Hydrodynamics*, 2nd Ed., Wiley, New York 1994.

[3] Bayraktar, T., Pidugu, S. B., *Int. J. Heat Mass Trans.* 2006, *49*, 815–824.

[4] Feng, P. X., *Surface Sci.* 1999, *429*, L469–L474.

[5] Rice, C. L., Whitehead, R., *J. Phys. Chem.* 1965, *69*, 4017–4024.

[6] Yang, C., Li, D. Q., Masliyah, J. H., *Int. J. Heat Mass Trans.* 1998, *41*, 4229–4249.

[7] Mala, G. M.,Yang, C., Li, D. Q., *Colloid Interface Sci. A* 1998, *135*, 109–116.

[8] Yang, C., Li, D. Q., *Colloids Surfaces A* 1998, *143*, 339–353.

[9] Zhang, Y. L., Wong, T. K., Yang, C., Ooi, K. T., *Int. J. Eng. Sci.* 2005, *43*, 1450–1463.

[10] Xuan, X. C., Li, D. Q., *J. Colloid Interface Sci.* 2005, *289*, 291–303.

[11] Rektorys, K., *Variational Methods in Mathematics, Science and Engineering*, 2nd Ed., Reidel, Dordrect 1980.

[12] Wang, C. M., Wang, L., Liew, K. M., *J. Sound Vibr.* 1994, *171*, 301–314.

[13] Hsu, J. P., Kao, C. Y., Tseng, S. J., Chen, C. J., *J. Colloid Interface Sci.* 2002, *248*, 176–184.

7 Appendix: Analytic solutions

For the circular tube, Eq. (3) in polar coordinate is

$$\phi_{rr} + \phi_r/r = K^2\phi \tag{A1}$$

The bounded exact solution with value 1 on the boundary is in terms of the modified Bessel function

$$\phi = \frac{I_0(Kr)}{I_0(K)} \tag{A2}$$

It is seen that for large K, the potential concentrates near the boundary, or from Eq. (4) the velocity is approximately uniform in the interior of the tube. Integration gives the normalized flow rate

$$\bar{Q} = 2\pi \int_0^1 (1-\phi) r\,dr = \pi\left[1 - \frac{2I_1(K)}{kI_0(K)}\right] \tag{A3}$$

Figure A1 shows the flow rate as a function of K. Using the asymptotic behaviors of the modified Bessel's functions for small and large K in Eq. (A3), one finds that $\overline{Q}$ initially increases as

$$\bar{Q} \sim \pi K^2/8 \text{ for small } K \tag{A4}$$

and then approaches π as

$$\bar{Q} \sim \pi\left(1 - \frac{2}{K} + \frac{1}{K^2} + \cdots\right) \text{ for large } K \tag{A5}$$

For a rectangular conduit, let the normalized width be 2 and the height be $2b$ and set Cartesian axes at the center. The solution to Eq. (3), 0 at $y = \pm b$ and unity at $x = \pm 1$ is

$$\phi_1 = \sum_{n=1}^{\infty} a_n \cos(\alpha_n y) \frac{\cosh\left(\sqrt{\alpha_n^2 + K^2}\,x\right)}{\cosh\left(\sqrt{\alpha_n^2 + K^2}\right)} \tag{A6}$$

where $\alpha_n = (n - 1/2)\pi/b$ and a_n is the Fourier coefficient of unity $\alpha_n = 2(-1)^{n+1}/(b\alpha_n)$. A similar solution satisfies zero boundary conditions at $x = \pm 1$. The total solution is thus

$$\phi = \sum_1^{\infty} \left[a_n \cos(\alpha_n y) \frac{\cosh\left(\sqrt{\alpha^2 + K^2}\,x\right)}{\cosh\left(\sqrt{\alpha_n^2 + K^2}\right)} + \right.$$
$$\left. + b_n \cos(\beta_{nx}) \frac{\cosh\left(\sqrt{\beta_n^2 + K^2}\,y\right)}{\cosh\left(\sqrt{\beta_n^2 + K^2}\,b\right)} \right] \tag{A7}$$

where $\beta_n = (n - 1/2)\pi$ and $b_n = 2(-1)^{n+1}/\beta_n$. The solution (A6) has also been derived by Yang and Li [8], but their form of velocity (and consequently flow rate) is in terms of a double infinite series in Green's functions. The series solution (A7) is now substituted in the solution form for the velocity (4) to obtain the much simpler form for the normalized flow rate, after straightforward integration

$$\bar{Q} = 4b - \sum_1^{\infty} \frac{8}{[(n-1/2)\pi]^2} \left[b \frac{\tanh\sqrt{\alpha_n^2 + K^2}}{\sqrt{\alpha_n^2 + K^2}} + \right.$$
$$\left. + \frac{\tanh\left(\sqrt{\beta_n^2 + K^2}\,b\right)}{\sqrt{\beta_n^2 + K^2}} \right] \tag{A8}$$

For large K, we find

$$\bar{Q} \sim 4b - \frac{b+1}{K} + O(K^{-2}) \tag{A9}$$

The normalized flow rate for a rectangle is given in Table A1 for comparison with future research. Five-digit accuracy is achieved when the series contains about 1000 terms.

Table A1. Normalized flow rate $\bar{Q}$ *vs.* K and b for rectangular channels

K/b	0.25	0.5	0.75	1
0.1	0.0001755	0.001143	0.003041	0.005612
0.2	0.0007014	0.004560	0.01211	0.02232
0.5	0.004363	0.02805	0.07357	0.1341
1	0.01716	0.1062	0.2674	0.4716
2	0.06440	0.3505	0.7875	1.2811
5	0.2819	1.0097	1.8042	2.6038
10	0.5552	1.4510	2.3510	3.2510
20	0.7628	1.7128	2.6628	3.6128
50	0.9021	1.8820	2.8621	3.8421
∞	1.0000	2.0000	3.0000	4.0000

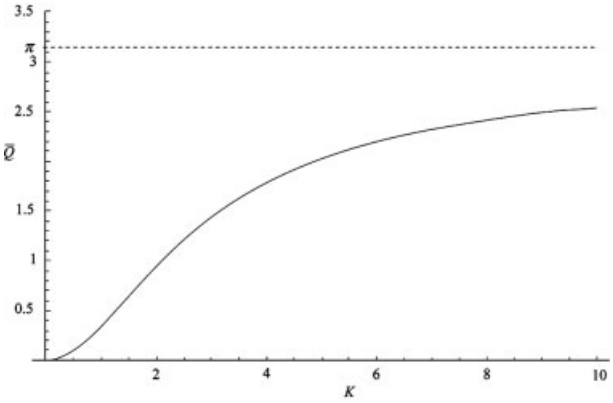

Figure A1. Normalized flow rate $\bar{Q}$ *vs.* the nondimensional electrokinetic width K.

